Study on the Reasonable Parameters of the Concentric Hemisphere-Style Shaped Charge for Destroying Rock

Trong Thang Dam[1](✉), Xuan-Nam Bui[2], Tri Ta Nguyen[1], and Duc Tho To[3]

[1] Le Quy Don Technical University, 236 Hoang Quoc Viet Ward, Bac Tu Liem District, Hanoi 100000, Vietnam
thangdt@lqdtu.edu.vn

[2] Hanoi University of Mining and Geology, 18 Pho Vien, Duc Thang Ward, Bac Tu Liem District, Hanoi 100000, Vietnam

[3] Vietnam Mechanics Association, 64 Doi Can Ward, Ba Dinh District, Hanoi 100000, Vietnam

Abstract. Currently, increasing the ratio of useful energy for external charge to destruct rock is a necessary research direction. Therefore, using an analytical method, this study established the dependence of the explosive force and the productivity of using energy for the concentric spherical shaped charge on the uniform-geometric characteristic parameters of this shaped charge. A computational programme was developed in the MATLAB software to calculate, investigate and analyse the abovementioned rule of dependence. The analysis and evaluation of this rule combined with the analysis of the purpose of the rock obstacle destruction allow to select reasonable uniform-geometric characteristic parameters of the concentric hemisphere shaped charge. The model is designed and created for selected concentric hemisphere shaped charge to fill 40 g of plastic explosive C4. The surface of the inner hemisphere of this shaped charge is a hemisphere lining funnel that is made of steel with a thickness of 1 mm. Tests were conducted, and the explosion efficiency of the concentric hemisphere concentrated shaped charge model was compared with that of the normal concentrated charge with the same 40-g explosive amount. The obtained results show that the productivity of concentric hemispheres shaped charge is 2.7 times higher than that of the concentrated charge. Furthermore, in the experiments for grade M300 concrete samples, the destructive zone volume of the proposed hemispherical shaped charge was approximately 2 times higher than that of the conventional concentrated charge.

Keywords: Charge · Shaped charge · Destroy · Blasting rock · Concentric hemisphere

1 Introduction

Currently, during rock blasting work, the method of external charges is often used when borehole blasting is difficult to apply such as in deep excavation of the seabed under complex hydrological conditions and when the size of the project is not large or when

X.-N. Bui et al. (Eds.): ISRM 2020 - Volume 1, LNCE 109, pp. 45–68, 2021.
https://doi.org/10.1007/978-3-030-60839-2_3

breaking oversized rocks or breaking construction structures on land or underwater [1, 3, 4, 7, 8, 11, 12, 14–16]. The external charge method has low efficiency because most of the energy is lost into air or water [1, 5, 7, 8, 11, 15].

To improve the rock destruction efficiency of the concentrated external charge, the following solutions are available.

- Direction 1: Optimise the shape and the relative ratio among sizes of the concentrated charge. This direction is based on the harmony of the unit explosive pulse and the total explosive pulse of the explosive products impacting directly on the obstacle [1, 5, 6, 10, 21];
- Direction 2: Use layers of inert material such as soil, sand, or water to cover the charges to reduce the loss of explosive energy into the air and increase the energy transferred into the obstacle [7, 8, 11, 14, 15, 19–21];
- Direction 3: Design and apply different types of shaped charge to increase the useful energy to break obstacles [1, 2, 5, 8, 9, 11–16, 20]. This direction is mainly applied worldwide in the military for the purpose of cutting or piercing the obstacles made of steel or concrete; thus, the only criterion for evaluating the effect of breaking the obstacle is the depth of the cut; however, the width of the cut has to be as small as possible. Therefore, the volume of destruction is ignored [2, 5, 9, 11, 15]. However, for soil and rock destruction, the volume of the destruction area is considered to be the most important criteria for all types of charges [1, 17, 19].

The published research results on shaped charges to break the rock are limited and are mainly published in the form of commercial information. Examples include the Russian oversized rock blasting volumes, KZP-5, KZP-100, KZP-200, KZP-300, KZP-400 [13], and FRACMEX Nitro Nobel underwater shaped charge is used in Sweden and Spain [18]. Thusfar, there has not been a comprehensive theory on the soil destruction effect of shaped charge. The publication of calculation and experimental methods on shaped charges to destruct rock or soil has not been determined. Therefore, it is necessary to study solutions to use concentric hemisphere shaped charge to improve the rock destruction efficiency.

2 Analysing Theoretical Basis of Direct Mechanical Effects of Explosive Products

Typically, explosive detonation speed is very large (i.e., 5000–8000 m/s). Therefore, when studying the direct effect of explosive products on obstacles, it is possible to assume that the charge is immediately detonated. In addition, when explosion is performed in air, the air pressure can be ignored because it is smaller than the pressure of the explosive product at the start of bursting out. From the basic abovementioned assumptions, it can be assumed that the entire initial energy of the explosive is the potential energy when the exploded material has completely transformed into the kinetic energy of the explosive product. During an instant charge detonation, first, the explosive product completely occupies the volume of the charge prior to detonation, and all explosive particles are immobile. The movement of explosive product particles starts from the outermost layer

on the surface of the charge. Therefore, a surface appears between the moving explosive product element and the stationary element. This surface moves deeply into the charge at the rate called the splash surface. The movement speed of the splash surface during all splash times remains the same. Therefore, at each moment, the volume of moving explosive product will be similar to the initial volume shape of the charge.

Therefore, based on geometric characteristics, it is easy to observe explosive products flying in a certain direction. The interface between two adjacent splash surfaces is the bisectoral plane of two adjacent explosive surfaces. The ratio of the mass of explosive gas product that flies in a given direction and the total mass of charge is called the coefficient of explosive use in that direction (Fig. 1).

If the initial density at all points of the charge is the same, the coefficient of explosive energy use in a certain direction is [1, 2, 6, 10, 21]:

$$\eta = \frac{V_a}{V} \tag{1}$$

where: V_a - volume of the explosive product flying in the direction to be determined;

V - volume of the total charge;
η - coefficient of explosive energy use in a certain direction also known as explosive performance or the relative volume of the active charge.

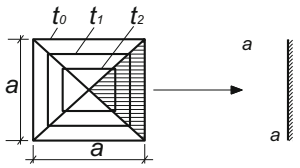

Fig. 1. Explosion product splash diagram of a cube charge t_0, t_1, t_2 - The location of the splash surface at three different times

Explosive products can only fly from the open side of an explosive. If any portion of the surface of the charge is in contact with an absolute hard and stationary obstacle, the explosive products will only fly in the direction of the remaining free surfaces.

By applying the laws of conservation of energy, the momentum and mass allow to determine the full impulse effect on the obstacle of the square-box bottom shaped charge with the length edge of b, height H, and the cylindrical charge with diameter b and height H [1, 5, 6, 10, 21]:

$$I = \sqrt{Q_o}\, C\mu \tag{2}$$

where: C - weight of the charge, kg;

Q_o - specific heat of the explosive, J/kg;
μ - factor of the form charge.

Thus, to increase the productivity of obstacle destruction, it is necessary to increase the explosion pulse applied to the obstacles. When the explosive type and weight is fixed, the explosive impulse propagating into the obstacle increases when the energy use coefficient increases in the direction of striking the obstacle. An increase in the use of explosive energy is made by changing the geometric structure of the charge.

Explosive theory has confirmed that [1, 5, 9, 10] when using external charges, if the concave surface with reasonable parameters is placed to face towards obstacles to be destructed, the destructive performance will be considerably improved.

3 Determining the Reasonable Congruent Parameters of the Shaped Charge

3.1 Establishing a Rule Depends on the Explosive Energy Efficiency of Concentrated Sphere–Shaped Explosive Volume with a Concentric Conical Cone

Based on the theory presented in Sect. 2, in a general case, the charge is a sphere that is shaped with concave spheres, spheres with concentric O, and concave bottom facing towards the required environment surface to be destructed (Fig. 2). The charge has a diameter of $D = 2R$, height $H = \overline{H}D$ ($\overline{H} = H / D$ relative height of shaped charge). The outer sphere has radius r_2, and the inner sphere has radius r_1.

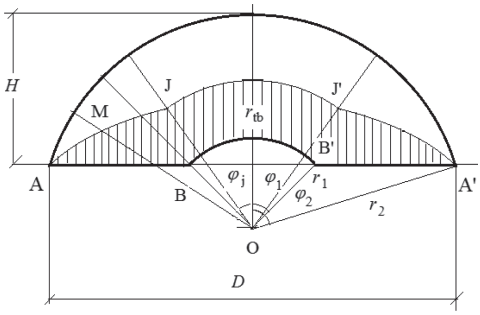

Fig. 2. Concentric spherical charge

Let r_p be the radius of the sphere that is spaced evenly inward and outward:

$$r_{tb} = \frac{r_1 + r_2}{2} \tag{3}$$

Let J be the point on the cross section of the charge, and the sphere is separated so that J is equidistant from the inner, outer and top surfaces of the charge. Thus, J is the intersection point of circle O with radius r_{tb} with the line that is parallel to AA′-spaced AA′ distance $\frac{r_1 - r_2}{2}$. The dispersion separator of the explosive product on the charge section is the curve AJJ′A′, where JJ′ is the centre circle O of the radius r_{tb}, and AJ and

J′A′ are the curves of points that are equidistant from the outer sphere and the top of the charge.

To establish geometric relations, the following relation is used:

$$H = r_2(1 - \cos\varphi_2) = \frac{D}{2\sin\varphi_2}(1 - \cos\varphi_2) = \frac{D}{2}\frac{2\sin^2\frac{\varphi_2}{2}}{2\sin\frac{\varphi_2}{2}\cos\frac{\varphi_2}{2}} = \frac{D}{2}\tan\frac{\varphi_2}{2}$$

$$\varphi_2 = 2\arctan\frac{2H}{D} = 2\arctan\left(2\overline{H}\right) \tag{4}$$

The radius of outer and inner spheres are:

$$r_2 = \frac{D}{2\sin\varphi_2}; \qquad r_1 = \eta_d r_2 \tag{5}$$

Inside: η_d relative bottom concave sphere radius is the ratio between the radius of the bottom sphere r1 and the radius of the outer sphere r_2, which are:

$$\eta_d = \eta_{gh} \div 1; \quad \eta_{gh} = \cos\varphi_2$$

From the relationship:
$r_2\cos\varphi_2 = r_1\cos\varphi_1$, get:

$$\varphi_1 = \arccos\left(\frac{r_2\cos\varphi_2}{r_1}\right) = \arccos\left(\frac{\cos\varphi_2}{\eta_d}\right) \tag{6}$$

From the position of J, the following relations are obtained:

$$r_{tb}\cos\varphi_j = r_2\cos\varphi_2 + \frac{r_1 - r_2}{2} = r_2\cos\varphi_2 + \frac{r_1(1 - \eta_d)}{2}$$

$$\cos\varphi_j = \frac{r_2(2\cos\varphi_2 + 1 - \eta_d)}{2r_{tb}}$$

$$\varphi_j = \arccos\frac{r_2(2\cos\varphi_2 + 1 - \eta_d)}{2r_{tb}} \tag{7}$$

Explosive volume:

$$V = V_{c2} - V_{c1} \tag{8}$$

Where:

$$V_{c2} = \frac{\pi}{3}r_2^3\left(2 - 3\cos\varphi_2 + \cos^3\varphi_2\right)$$

$$V_{c1} = \frac{\pi}{3}r_1^3\left(2 - 3\cos\varphi_1 + \cos^3\varphi_1\right)$$

Active explosive volume:

$$V_a = \int_{\varphi=0}^{\varphi_2} \pi(R_p\sin\varphi)^2 d(-R_p\cos\varphi) - V_{cl}$$

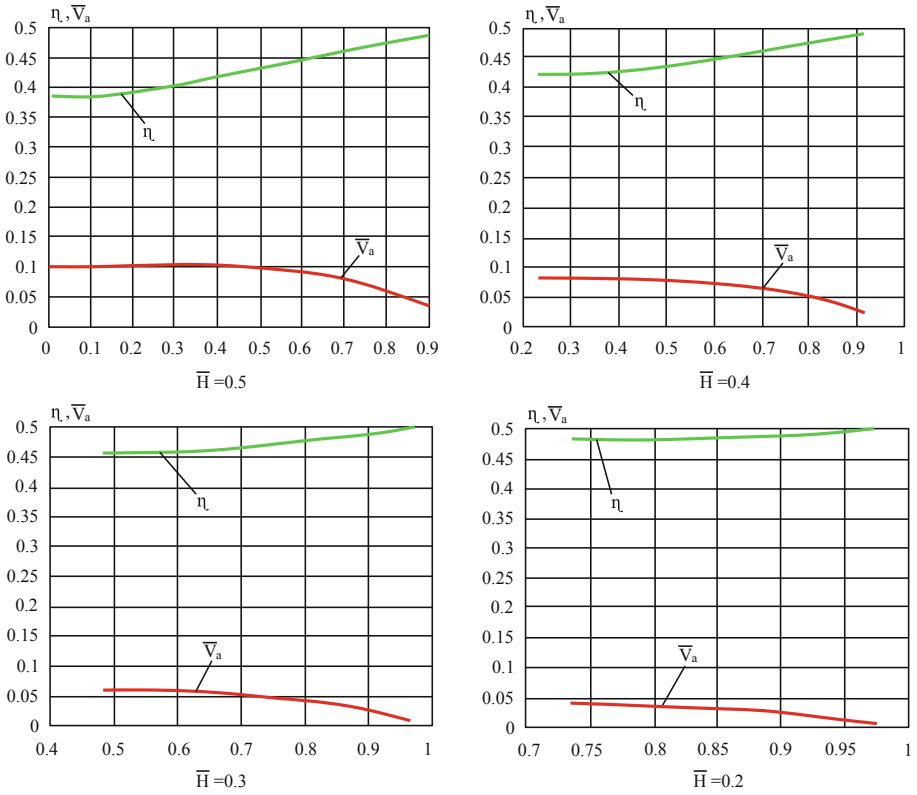

Fig. 3. Graph of the power and productivity of explosive use of concentric spherical charge

Where R_p is the distance from centre O to the separating surface of the explosive product. When, $\varphi \le \varphi_j$, $R_p = r_2$; when, $\varphi > \varphi_j$, $R_p = R_M$:

$$r_2 - R_M = R_M \cos\varphi - r_2 \cos\varphi_2$$

$$R_M = \frac{r_2(1+\cos\varphi_2)}{(1+\cos\varphi)}$$

$$d(R_M \cos\varphi) = -R_M \sin\varphi d\varphi + \cos\varphi dR_M$$

$$d(R_M \cos\varphi) = -\frac{r_2(1+\cos\varphi_2)}{(1+\cos\varphi)} \sin\varphi d\varphi + \cos\varphi \frac{r_2(1+\cos\varphi_2)}{(1+\cos\varphi)^2} \sin\varphi d\varphi$$

$$d(R_M \cos\varphi) = r_2(1+\cos\varphi_2)\left[\frac{\sin\varphi\cos\varphi}{(1+\cos\varphi)^2} - \frac{\sin\varphi}{(1+\cos\varphi)}\right] d\varphi$$

We obtain:

$$V_a = \pi r_{tb}^3 \int_{\varphi}^{\varphi_j} \sin^3\varphi d\varphi + r_2(1+\cos\varphi_2) \int_{\varphi=\varphi_j}^{\varphi_2} \pi\left(R_p \sin\varphi\right)^2 \left[\frac{\sin\varphi}{(1+\cos\varphi)} - \frac{\sin\varphi\cos\varphi}{(1+\cos\varphi)^2}\right] d\varphi - V_{c1}$$

$$V_a = V_{cj} - V_{c1} + \pi r_2^3 (1 + \cos\varphi_2)^3 \int_{\varphi=\varphi_j}^{\varphi_2} \frac{\sin^3\varphi}{(1+\cos\varphi)^3}\left[1 - \frac{\cos\varphi}{(1+\cos\varphi)}\right] d\varphi \quad (9)$$

Inside: $V_{cj} = \frac{\pi}{3} r_{tb}^3 \left(2 - 3\cos\varphi_j + \cos^3\varphi_j\right)$

The productivity of explosive energy use is the coefficient of using explosive energy in that direction, which is determined by formula (1).

The force of the charge applied to an obstacle (referred to as the force of the charge) is characterised by the relative volume of the active explosive block [2, 4]:

$$\overline{V_a} = \frac{V_a}{D^3} \quad (10)$$

The general force of the charge impacting on an obstacle is characterised by its relative volume [2, 4]:

$$\overline{V} = \frac{V}{D^3} \quad (11)$$

The formulas (8) to (11) can be unified to the diameter of the charge D. Thus, the explosive uses a factor that depends only on two parameters $\overline{H}$ and η_d, where $\overline{V} < 0,\ 5$ and $\eta_d = \eta_{gh} \div 1$.

Figure 3 shows the power and productivity of explosive energy using different values of numbers and η_d.

The graph in Fig. 3 shows that:

- Explosive power varies inversely with explosive performance;
- The bigger is the concave (η_d big), the more efficiently the charge increases and the more explosive power it decreases;
- The higher is the height of the charge, the higher is the explosive power and the lower is the efficiency of the charge.

3.2 Analysis and Selection of Reasonable Uniform Parameters of the Concentric Concave Spherical Charge

The comparison of this concentric spherical cone-shaped shape charge model with the research results of the cylindrical concave explosion model with the conical concave funnel [4] allows us to make the following conclusions:

The powerful concentric spheroidal blasting form (Fig. 2) of the active charge fraction (the relative volume of the active charge, $\overline{V}_a$) is less than 0.1; however, the efficiency (coefficient of using explosive energy, η) is usually higher than 0.4 (see Fig. 3). The force of active detonation is the highest when the detonation height is equal to half of the detonation diameter (detonation size); then, the outside of the explosive quantity is the highest, i.e., hemispherical.

The shape charges used to cut steel focus only on creating holes deeply into the obstacles; the smaller is the hole width, the better the charge performs. These types of shape charges are usually designed to ensure that the charge base is located far away, i.e.,

2-3 times the obstacle diameter of the charge. This distance is called the focal length. The obstacle breaking principle of this shape charge is based on the kinetic effect of the penetrating flow formed from the lining hopper into the obstacle [1, 2, 5, 9, 17]. Compared to the concave blasting volume for steel cutting, the shape charge used in rock breaking needs to harmonise both the kinetic effects of the penetrating flow and the explosive product pressure, which is the shock wave pressure acting on the obstacle. The criterion for evaluating the effectiveness of rock breaking is the general volume of the destruction zone. Thus, if the principle of steel cut concave blasting used to break rock is applied, the efficiency will be very low.

The above-mentioned analysis shows that to improve the rock breaking efficiency of concentric spherical shaped charge, this type of charge structure is chosen not only to harmonise the power factor and explosion efficiency, but also the design of the structure closer to the obstacle surface to enhance the effect of the shockwave and explosive product pressure on the obstacle.

For the hemisphere charge, to make the power and distance to the obstacle surface (stone slabs) as small as required by the above-mentioned analysis, it is best to choose the concentric spherical charge with the highest height $\overline{H} = 0.5$. According to the graph in Fig. 3, the parameters are selected in the region:

$$\overline{H} = 0.5;\ \eta_d = 0.6\ldots 0.7;\ \eta = 0.45\ldots 0.46;\ \overline{V}_a = 0.09\ldots 0.08.$$

Thus, we can obtain and analyse one of the following five cases, with the same parameters described in Table 1.

Table 1. Identical parameters of concentric hemispherical charge

TT	Parameters	CA1	CA2	CA3	CA4	CA5
1	Relative bottom concave sphere radius η_d	0.6	0.62	0.64	0.66	0.68
2	Relative height of charge $\overline{H}$	0.5	0.5	0.5	0.5	0.5
3	Relative volume of charge $\overline{V}$	0.2053	0.1994	0.1932	0.1865	0.1795
4	Force of a charge $\overline{V}_a$	0.0914	0.0894	0.0872	0.0847	0.0820
5	Productivity of explosive η, %	44.54	44.83	*45.12*	45.42	45.70

Natural rocks have properties that vary in a wide range with 4 levels, which correspond to the solidity ranges from 1 to 20. For the optimum rock breaking effect, an appropriate charge needs to be chosen for each type of rock or mine. The analysis of the above-mentioned 5 cases shows that an increase in explosive power and mine performance has an inverse relationship.

The stronger is the rock, the stronger is the explosive force and vice versa. Therefore, for practical applications, this study chooses case 3 as the semi-concentric shaped charge to be tested on the model.

According to case 3, the productivity of concentric shape charge is 45.12%, which is 2.7 times higher than that of concentrated charge with the same mass (the optimal

concentration charge has a diameter that is twice the height and efficiency of 16.7%). However, the productivity of rock destruction of the shaped charge, besides the dependence on the efficiency and power of the shaped charge, also depends on the momentum of the penetrated metal flowing formed from the conical cone. Therefore, the combined efficiency of the shaped charge and concentrated charge should be compared and evaluated through experimental results.

4 Experimental Framework

4.1 Purpose

- Compare the destructive volume of the test sample of the concentric hemisphere shape charge to that of the concentrated charge with the same mass;
- Compare stress and deformation values in the sample of concentric hemisphere on cave charge compared to the concentrated charge with the same mass.

4.2 Describe the Experimental Model and the Method of Conducting the Experiment

The Experimental Model Includes the Following. The concentric hemisphere shape charge is designed in the form of a miniature model containing 40 g of flexible plastic explosive C4 with properties shown in Table 2; the geometric structural parameters of concave mines are described in Table 3 and Fig. 4 below. The shape charge is made of an aluminium shell to ensure a smaller impact of the durability of the shape charge on

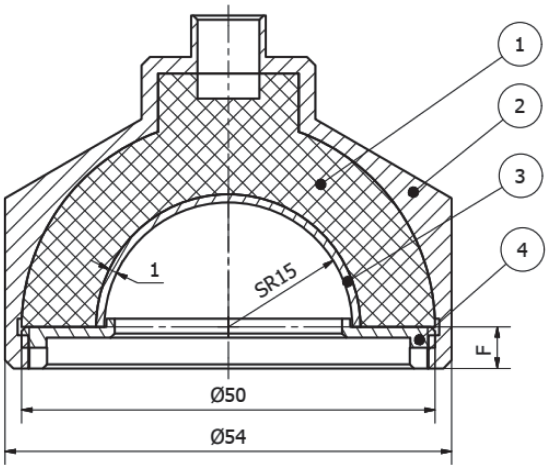

Fig. 4. Design drawing of the concave hemispherical concentrated charge model 1. Plastic explosive C4; 2. Concave explosive aluminium shell; 3. The hemispherical lining funnel is made of steel; 4. The ring holding hopper liner

the explosive effect; the hemispherical lining funnel is made of a 1-mm thick CT3 steel. The shell details of the concave explosion and hemispherical lining funnels are made by the lathe method on CNC equipment. The geometrical parameters of concave explosion quantity are shown in Table 3 and Fig. 3.

Table 2. Characteristics of the C4 plastic explosive

No	Parameters	Unit	Values
1	Moisture content and volatile matter	%	≤0.3
2	Flexibility (Needle penetration at 25 °C, uncompressed drug forming cakes)	10^{-1} mm	44–85
3	Impact sensitivity	%	8–32
4	Density	g/cm^3	1.45–1.64
5	The ability to reproduce according to the magic pendulum	%TNT	116–136
6	Explosive speed (at density of 1.45 g/cm^3)	m/s	7300–7700
7	Lead cylinder pressure (25 g, density 1.45 g/cm^3)	mm	≥22

Table 3. Comparison of dimension parameters of concentric spherical charge and concentrated charge containing 40 grams of C4

No	Parameters	The concentric spherical charge	The concentrated charge
1	η_d	0.64	–
2	D, mm	50	D = 2H
3	H, mm	23.5	
4	r_1, mm	15	–
5	η, %	45.12	16.7
6	Force of a charge, $\overline{V_a}$	0.0872	0.261

– The amount of control concentrated charge is also 40 g of C4 plastic explosive with the parameters listed in Table 3. The concentrated charge is placed in a plastic pipe. The two ends of the explosive were left open.
– The shaped charge is made of an aluminium shell, a 1-mm-thick steel funnel; the geometric parameters of the concave pillar explosion are shown in Table 3.
– The material to be demolished is an M300 concrete sample with the size of 40 × 40 × 40 cm.
– A set of concrete deformation measuring instruments includes: strain gauge PL-60-11 from Japan (Tokyo Sokki Kenkyujo Co., Ltd) (see Fig. 5a) and a multichannel oscilloscope CSI-1000DC National Instruments (NI) from the USA, which has 24 channels and the maximum frequency of 200,000 signals/sec (see Fig. 5b). Strain

gauges are connected to a multichannel oscilloscope to receive distortion signals as a function of time after detonation.

a)

b)

Fig. 5. A set of measuring instruments for the deformation of concrete samples a. Multichannel oscilloscope measurement CSI-1000DC; b. Strain gauge PL-60

Method of Conducting the Experiment. We measured the destruction areas after explosion to compare and evaluate the destruction effect of soil and rock by shape charge to the concentrated charge. The instrument was used to measure the dimensions of the destruction areas by a ruler with millimetre accuracy.

Strain gauges (PL-60 paste 10 cm) were used to assess the effect of load increase when detonating a shape charge compared to the concentrated charge from the concrete sample surface.

Accordingly, strain gauge 4 were applied to concrete samples used to test the amount of concave explosion. Strain gauges 1 and 3 were arranged horizontally and glued to the concrete sample on two symmetrical sides of the concrete sample, while strain gauges 2 and 4 were arranged vertically along the specimen and stuck to the concrete sample on the remaining two symmetrical sides of the concrete sample (Fig. 6).

Meanwhile, strain gauge 2 was applied to the concrete samples used for concentrated charge control. Strain gauge 5 was arranged horizontally, while strain gauge 6 was arranged vertically along the specimen. Both were attached to the two symmetrical sides of the concrete sample (Fig. 7).

Before applying the strain gauges to the concrete samples, the part where the strain gaugepaste was placed was cleaned to smoothen the concrete surface and ensure that the sensors attached to the concrete samples well contacted and adhered to the surface of the concrete samples during explosion. This was to ensure that the true deformation value of the concrete sample was obtained.

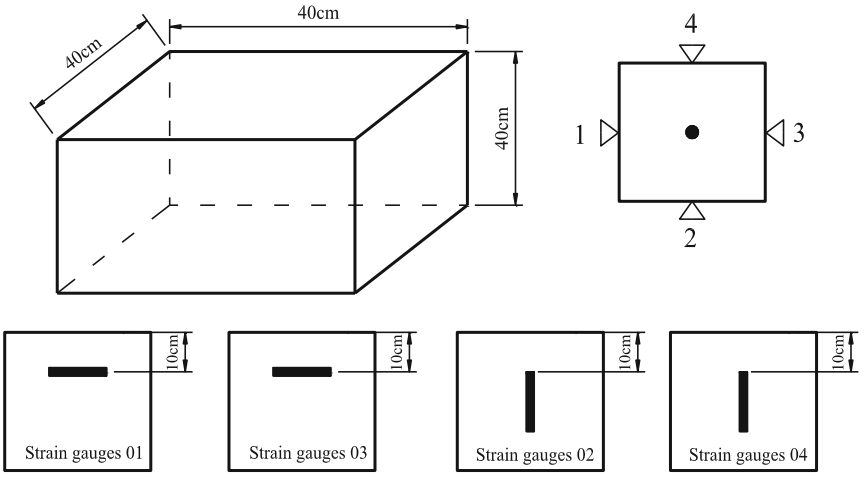

Fig. 6. Diagram of deformation sensors on a sample explosive for the explosion of the concave concrete sample

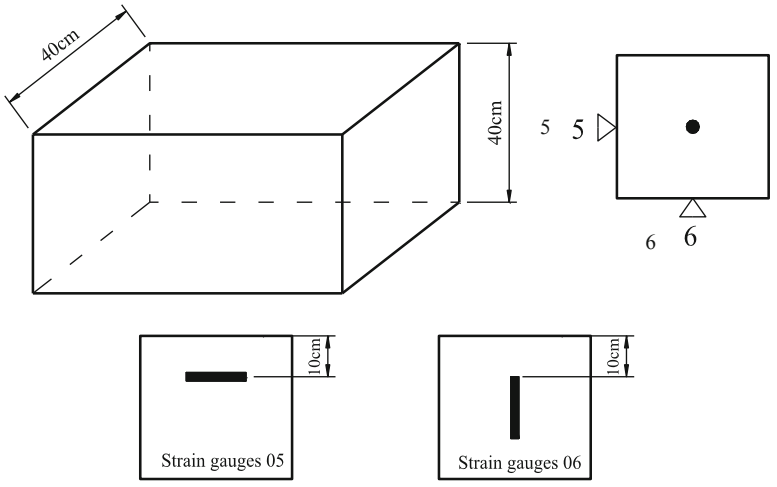

Fig. 7. Diagram of the deformation sensor on the explosive for the test explosion of the concentrated sample

The strain gauges were placed horizontally to consider the effect of the explosion on the deformation and stress of the specimen in the horizontal direction of the sample surface and vertically to consider the effect of the explosion on the deformation and stress of the sample along the sample surface.

During testing, the amount of concave explosion was arranged in the explosive surface at 5 mm distance from the concrete sample surface to ensure the mechanical design of the shell structure. Moreover, the optimal amount of explosive for the explosion must be tested at other distances to determine the optimal focal length. The concentrated

charge will be arranged in the explosive surface in direct contact with the concrete sample surface.

Each test charge (i.e., shape and concentrated charges) was placed on the concrete sample surface (Fig. 8) following the procedure below:

- Perform the detonation with electric detonator No. 8.
- After each explosion, measure the size and the volume of the destruction funnel on the sample surface with a ruler. Count the number of cracks and measure their depth.
- The number of testing samples includes 3 concrete samples using explosive tests corresponding to 3 shape charges, of which 01 concrete sample is used to measure deformation, and 3 concrete samples using explosive test corresponding to 03 concentrated charges of control focus, including one sample for the deformation measurement.

4.3 Experimental Results

Sample Destruction Areas. The results after the explosion showed that the test area received the effects of destroying the concrete samples of the concave and concentrated explosions, both of which have the following general form:

- In the position in direct contact with the concave or concentrated charge, the destruction area had the form of an explosion funnel. Radial cracks appeared around the mouth of the funnel. Many cracks extended to the side surface of the sample and along the concrete body (Figs. 8 and 9).
- Destruction funnel area: This area is a strong demolition-zone concrete shot out of the sample to master the demolition area in the shape of a funnel. This area is formed by the direct effect of the explosive pulse and the compressive stress in the explosion wave symbolised by index 3 in Fig. 8.
- Cracking area: This area shows cracks denoted by symbols 5 and 6 in Fig. 8. These fractures are formed by the components of the effect of the tangential tensile stress in the explosion wave formed around the explosion funnel. The volume of this region is calculated to include a strong destruction zone.
- The destruction characteristics of the concrete samples include the volume of the cracking area, area of cracks caused by fracture, number of cracks around the crater, crack depth along the body, and crack width in each explosive pattern. Table 3 depicts the results.

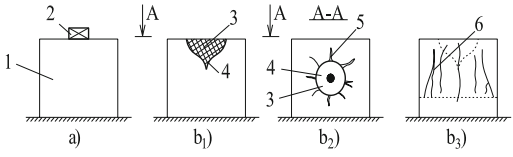

Fig. 8. Experimental diagram (a) and shape of areas of failure after explosion (b1, b2, and b3): 1) concrete sample M300; 2) location of the concave or concentrated charge; 3) funnel demolition; 4) piercing hole; 5) cracks on the face; and 6) cracks on the side

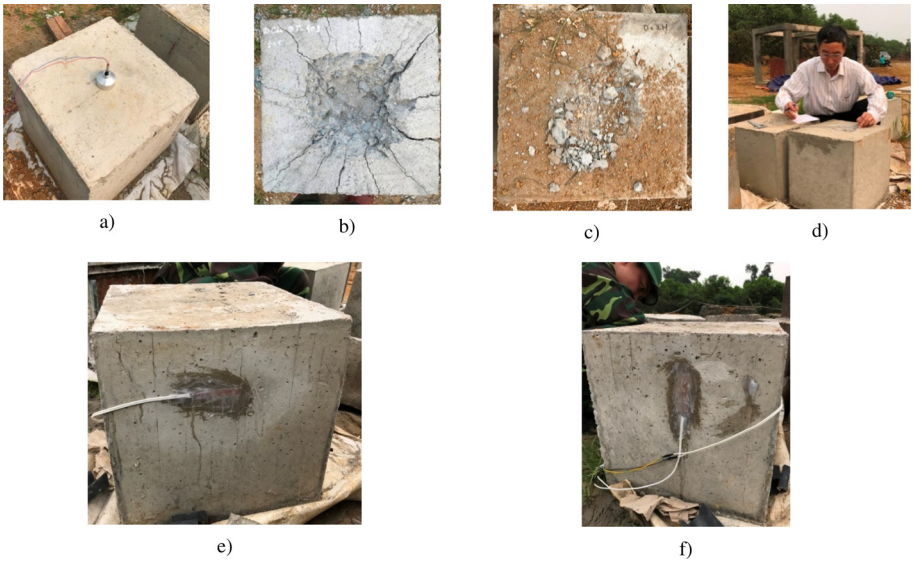

Fig. 9. Some images of experimental explosion: a) sample before explosion; b) sample after explosion by shape charge; c) sample after explosion by concentrated charge; d) data taking after the explosion; e) strain gauge attached to the concrete sample horizontally; and f) strain gauge attached to the concrete sample vertically

Table 4. Demolition-zone characteristics

TT	Type of charge, experimental conditions	The volume of the funnel area destroyed, Vn (cm^3)	Total number of cracks around the surface, N(cracks)	Crack depth/Crack width, $L_n/б$(cm)	Volume of the fractured area in comparison, V_k (cm^3)
1	The shape charge is located at a distance 5 mm	2,360	14	15–18/≤0.3	26,400
2		2,727	13	13–19/≤0.1	25,600
3		3,109	15	14–20,4/≤0.2	27,200
The average value		*2,732*	*14*	*16.6*	*26,400*
1	The concentrated charge to compare is located close to the obstacle	390	8	7–9/Mini-crack	12,800
2		400	7	8÷10/Mini-crack	14,400
3		380	6	6÷11/Mini-crack	13,600
The average value		*390*	*7.0*	*8.5*	*13,600*

Deformation Values on the Concrete Slope Surface

Cracks appeared at the glued position of strain gauges 4 and 6 on the concrete sample after the explosion. On the contrary, at the glued position of strain gauges 1, 2, 3 and 5, no cracks were observed in the concrete sample after the explosion.

Table 5 and Figs. 10 and 11 present the results of the deformation measurement obtained after the shape charge and concentrated charge experiments.

The time relative strain ε (t) has the following characteristics:+ point with strain value '0' corresponding to the time before explosion;+ score of the corresponding maximum relative strain value ε1 during the explosion impact; and + the point has the smallest relative strain value after the impact of explosion ε2.

To analyse the mechanical and physical properties of the explosion impact process of the concrete sample, we included the stress and the specific energy quantities corresponding to the strain values obtained in the test.

The dynamic stress value was calculated by the following formula:

$$\sigma = E_d.\varepsilon, \text{ Mpa} \tag{12}$$

where, ε is the relative strain value at the survey point; E_d is the dynamic elastic modulus of the concrete sample material used in the experiment determined as $E_d = k_d . E_s$; E_s is the static elastic modulus of the concrete sample material used in the experiment for the concrete graded M300; $E_s = 35{,}000$ MPa; k_d is the dynamic coefficient; and $k_d = 1.1–1.15$. $k_d = 1.1$ is chosen according to [22]. Table 5 presents the calculation results.

Table 5. Results of the relative strain measurements and the calculated stress values

Strain Gauges title	Dynamic modulus of concrete E (MPa)	Maximum (Peak)		Ending Blast		Times of deformation	Unit energy	Note
		Relative deformation, ε1	Stress value calculated, σ (MPa)	Relative deformation, ε2	Stress value calculated, σ (MPa)	τ1/ τ2 (ms)	W/ ΔW (kJ/m^3)	
The experimental shape charge								
Strain Gauges1	3.85E+04	0.00070573	27.17	0.000498577	19.195	43/265	9.59/ 4.80	
Strain Gauges 3	3.85E+04	0.000871042	33.539	0.000860864	33.143	48/224	14.61/ 0.34	
Strain Gauges2	3.85E+04	0.001882254	72.468	0.000217564	8.371	27/152	68.20 /67.29	
Strain Gauges4	3.85E+04	0.009248257	356.059	0.009248257	356.059	2/-	1646.46/ 0.00	Appear cracks through the Strain Gauges
The experimental concentrated charge								
Strain Gauges5	3.85E+04	0.009014276	347.05	0.009014276	347.05	2/-	1564.20/ 0.00	Appear cracks through the Strain Gauges
Strain Gauges6	3.85E+04	0.000846098	32.571	0.000298204	11.484	61/481	13.78/ 12.07	

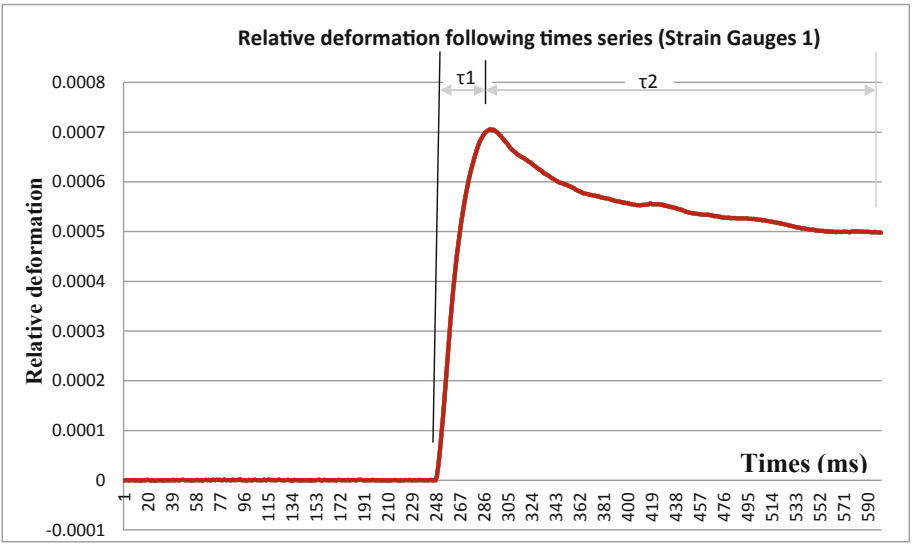

a)

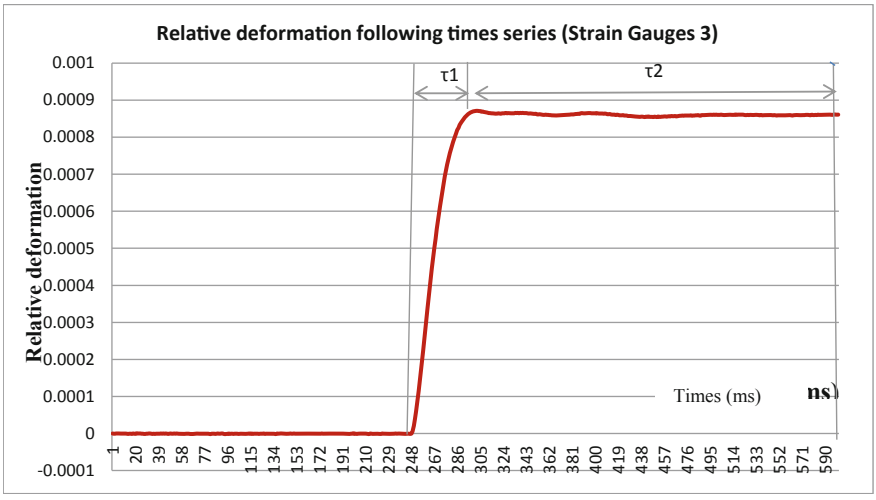

b)

Fig. 10. Relative deformation diagram of the concrete sample received during the shape charge explosion: (a, b) strain gauge 1 and 3 horizontally attached to the concrete sample; and (c, d) strain gauges 2 and 4 attached vertically to the concrete sample

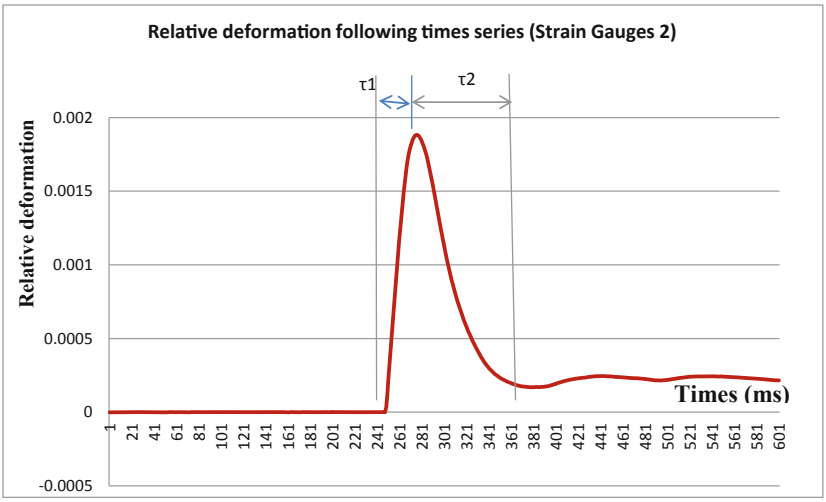

c)

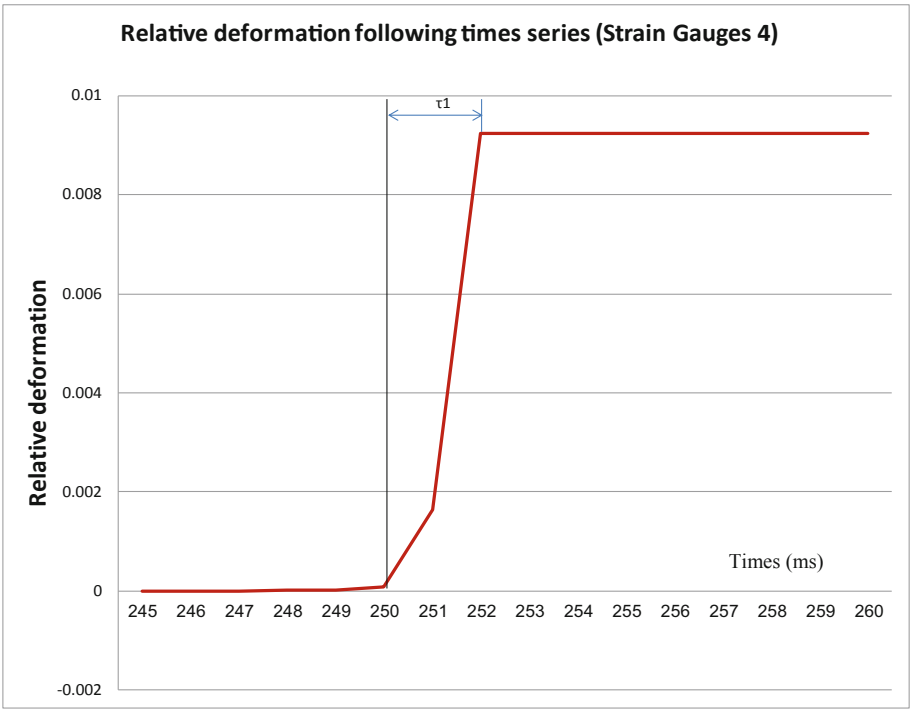

d)

Fig. 10. (*continued*)

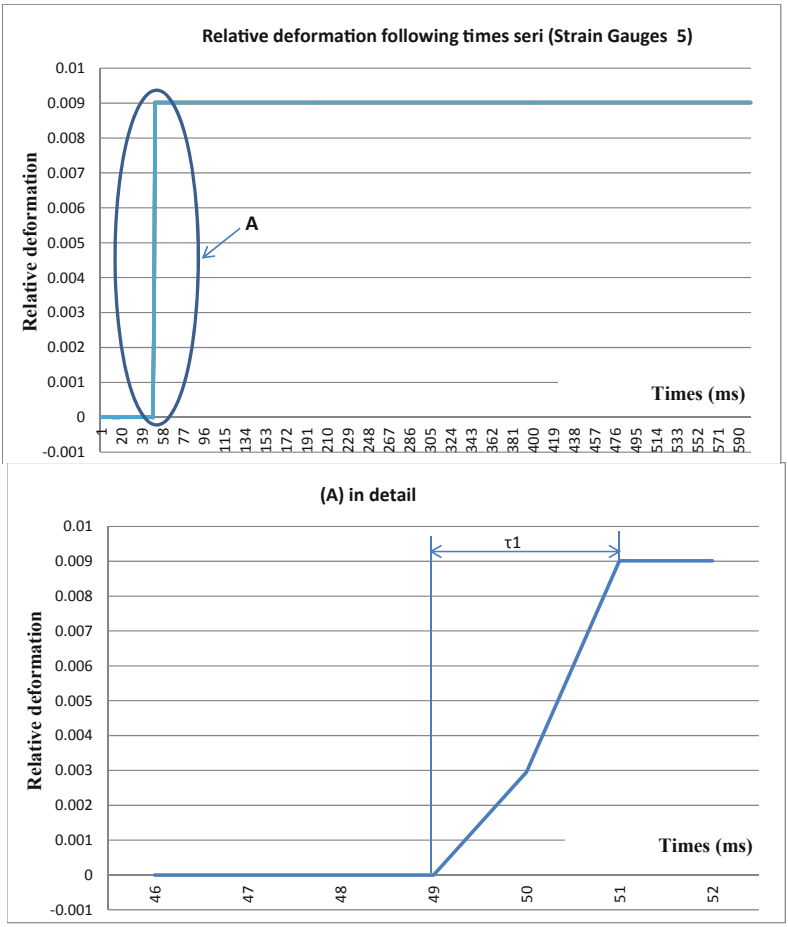

Fig. 11. Relative deformation diagram of the concrete samples received when the explosive concentration is concentrated: a) strain gauge 5 horizontally adhering to the concrete pattern and b) strain gauge 6 vertically attached to the concrete sample

The energy (W) in the detonation stress wave transmitted to the concrete sample to reach the maximum relative strain value is calculated as follows:

$$W = \frac{1}{2} E_d . \varepsilon^2 \tag{13}$$

The maximum value of the specific explosion energy (W) transferred to the concrete sample at the position of strain gauges is the energy value used to reach the maximum relative strain value ε1. The maximum specific energy value is calculated using as follows:

$$W = \frac{1}{2} E_d . \varepsilon_1^2 \tag{14}$$

Table 5 lists the calculation results W corresponding to the maximum relative strain value.

The part of the specific energy recovered from the maximum strain value ε1 to the value ε2 reflects the elastic potential of the concrete sample material in the explosion test (ΔW) calculated as follows:

$$\Delta W = \frac{1}{2} E_d . (\varepsilon_1^2 - \varepsilon_1^2) \tag{15}$$

Table 5 shows the calculation results ΔW.

5 Analysis of Experimental Results

Using the Excel section, we analysedthe data set in Table 4 in terms of the volume of the concrete demolition areas shown in the graphs in Fig. 12.

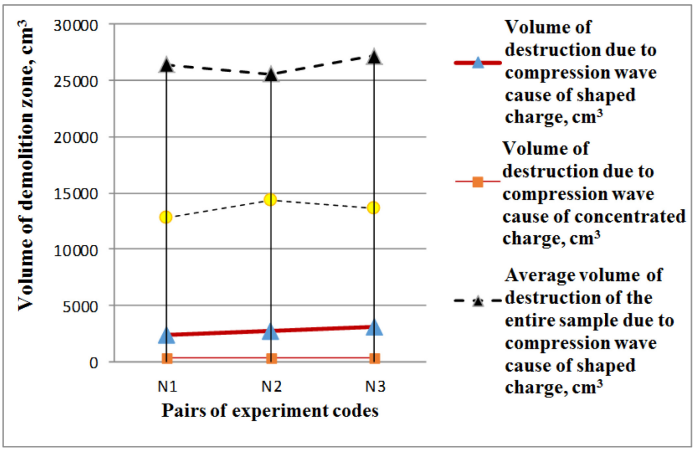

Fig. 12. Graph of the two cases for testing the concentric hemispherical and concentrated charges according to the volume of the destruction zone caused by compression and drag waves

The analysis of the data in Table 4 and the graph in Fig. 12 showed that when detonating an explosion at a focal length of 5 mm, the destructive efficiency caused by the concentric hemispherical concave was approximately 2 times more effective in the area volume demolition funnel and 2 times in the volume of the fractured area in comparison with the corresponding volume of the concentrated explosion. The average number of the cracks and crack depth was approximately 2 times higher than that of the concentrated charge.

The data analysis in Table 5 and the graph in Figs. 10 and 11 draw the following conclusions:

- The calculated deformation values and the stresses received by strain gauge 6 when measuring the transverse deformation and pasting the samples both received positive values. This result reflects the calculated stress values as tensile stress. As regards the law of explosive mechanics, these stress values are the tangential tensile stress components of explosive waves.
- The rule of the relative deformation change for all the strain gauges versus time has a common form: the relative deformation ε increases from '0' (initial value) to the maximum value (ε1) in a very short period (τ1) of about some milliseconds to some 10 ms. During the time after the relative deformation reached the maximum value, one of the two following cases can happen at each location of the strain gauges:

  - Case 1: Relative deformation continues to keep the maximum value, indicating that the saturation value has not changed over time. The horizontal strain curve is ε (t) = ε1 = maximum = constant. This includes strain gauges 4 and 5. The corresponding maximum values of stress and the corresponding maximum specific energy values of strain gauges 4 and 5 are 356.059 MPa, 1646.46 kJ/m^3 and 347.5 MPa, 1564.20 kJ/m^3, respectively. The values of the elastic strain potentials of the concrete sample materials in the explosion test (ΔW) of strain gauges 4 and 5 are equal to 0. The analysis of the obtained relative strain graph of strain gauge 4 in the concave explosion test (Fig. 10d) and strain gauge 5 in the reference focused explosion test (Fig. 11a) showed that the relative strain value reached the maximum value when the strain increased in very short period of time τ1 = 2 ms. The relative strain value reached saturation the whole time the zone was greater than 2 ms. We observed cracks of the concrete sample cut across the two locations of strain gauges 4 and 5. This reflects that at these locations the effect of the blast stress wave exceeded the strength of the concrete sample, thereby forming a deformation zone beyond the elastic and plastic thresholds. Therefore, although strain gauge 4 was used in the concave blast test (Fig. 10d), strain gauge 5 was used in a controlled concentrated blast explosion test with two independent concrete samples corresponding to two attached different strain gauges to the concrete sample in both vertical and horizontal directions. Note, however, that the resulting maximum relative strain values were almost identical (ε1 = 0.009248257 and 0.009014276).
  - Case 2: The relative strain decreased from the maximum value ε1 to the value ε_2 corresponding to time period τ_2. After time 2, the relative deformation reached the saturation value that did not change over time. This was a horizontal curve computed as ε (t) = ε_2 = minimum = const. In this case, the pairs of the maximum stress

values and the corresponding maximum specific energy values for strain gauges 1, 2, 3 and 6 were 27.17 MPa, 9.59 kJ/m^3; 72.468 MPa, 68.20 kJ/m^3; 33,539 MPa, 14.61 kJ/m^3; and 32,571 MPa, 13.78 kJ/m^3, respectively. The values of the potential elastic strain of the concrete sample materials in the explosion test (ΔW) of strain gauges 1, 2, 3 and 6 were 4.48 kJ/m^3, 67.29 kJ/m^3, 0.34 kJ/m^3, and 12.07 kJ/m^3, respectively. We analysed the obtained relative strain plots of strain gauges 1, 2, and 3 in the concave explosion test (Figs. 10a, b and c) and strain gauge 6 in the reference concentration burst test (Fig. 11b). The relative strain value reached the maximum value in the time of strain increase $\tau 1 = 27$–61 ms and the entire next time zone from $\tau 1$ to τ_2 (152–481 ms) relative deformation decreasing from the maximum value ε_1 to the value $\varepsilon 2$ and after the time $\tau 2$, the relative strain $\varepsilon 2$ does not change over time. At the two locations, no cracks appeared at the concrete sample cut across strain gauges 1, 2, 3 and 6. The relative strain recovery from the maximum value $\varepsilon 1$ to the value 2 reflected at the location of these strain gauges, the concrete sample is not destroyed. The relatively saturated strain 2 = const at times greater than $\tau 2$ denotes the irreversible plastic deformation zone, while the relative strain value ε_2 is the residual strain in the concrete sample after the operation was completed. We then analysed the change of the relative strain graph over time when the relative strain value reached its maximum (i.e., it still appeared in the time zone $\tau 2$ of strain Gauges 1, 2, 3 and 6). The convex and concave points are the sub-maximum and minimum points, respectively, appearing in the process of reducing the relative strain from $\varepsilon 1$ to $\varepsilon 2$. Gauges 6 and 2 in Figs. 11 and 10 showed the most obvious points, reflecting the recovery process to a semi-head state of concrete when deformed beyond the elastic threshold under the effect of load. Gravity is the process of diminishing oscillation. The value of the relative residual strain $\varepsilon 2$ reflects the intensity of the explosion stress wave acting at the survey point.

The range of the relative deformation of strain gauge PL-60 was 0.02. The maximum relative deformation gained of strain gauges 4 and 5 was also less than 0.02. Therefore, the maximum specific energy obtained at the crack location in the concrete sample (strain gauges 4 and 5) was reflected as the limited value of the specific energy required to destruct the concrete sample material graded M300. To verify this problem, we must perform a comparative analysis with the explosive index required for the destruction of the concrete sample material by explosion. The specific energy of the explosive number 6 ammonite was Qv = 1028 kcal/kg = 4307 kJ/kg. Thus, the calculated maximum specific energy values of strain gauges 4 and 5 (i.e., 1646.46 kJ/m^3 and 1564.20 kJ/m^3, respectively) were converted equivalent to the unit ammonite consumption of 0.38 kg/m^3 and 0.36 kg/m^3 respectively. The tested concrete sample graded M300 had a compressive strength of 30 MPa (300 kg/m^2). This strength was equivalent to the conglomerate rock in the rock classification table with the unit explosive consumption value of ammonite 6 as 0.35-0.45 kg/m^3 when blasting [17, 19]. This result coincides with the calculated unit ammonite explosive consumption converted from the experiment, confirming that the maximum specific energy value corresponding to the case of the crack is the critical specific energy required to destruct the M300 concrete sample.

Comparing the maximum relative strain value or maximum tensile stress value in the corresponding non-destructive area of concrete when detonating the shape charge

(strain gauge 2) with the explosion of the concentrated charge (strain gauge 6) draws the following result:

$$\frac{\varepsilon_{1.2}}{\varepsilon_{1.6}} = \frac{\sigma_{1.2}}{\sigma_{1.6}} = \frac{0.001882254}{0.000846098} = \frac{72.468\text{Mpa}}{32.571\text{Mpa}} \approx 2.2 \tag{16}$$

where, $\varepsilon_{1.2}$ and ε_1 are the maximum relative strain values obtained from strain gauges 2 and 6, respectively, and $\sigma_{1.2}$ and $\sigma_{1.6}$ are the calculated maximum stress value corresponding to the corresponding maximum relative strain value of strain gauges 2 and 6, respectively.

Comparing the corresponding maximum specific energy value of concrete when detonating the shape charge (strain gauge 2) with the concentrated charge (strain gauge 6) yields:

$$\frac{W_{1.2}}{W_{1.6}} = \frac{\varepsilon_{1.2}^2}{\varepsilon_{1.6}^2} = \frac{68.20\text{ kJ}}{13.78\text{ kJ}} = \frac{0.001882254^2}{0.000846098^2} \approx 4.5 \tag{17}$$

in which: $W_{1.2}$, $W_{1.6}$ is the corresponding maximum specific energy value of concrete when detonating the shape charge (Strain Gauges 4) compared with concentrated charge (Strain Gauges 6) respectively.

From the comparative analysis of the results of the destruction volume area and the stress–deformation value of the concrete samples (i.e., when the hemispherical shape charge is compared with the control concentrated charge), the concentric spherical shape charge will destruct by approximately 2 times the destructive power of the concentrated charge with the same explosive mass. This research result is consistent with that obtained by Professor A.N. Khanukaev of the Leninsky Mining Institute of Russia: 'stress wave parameters appear in granite under the effect of concave explosion with hopper lining in almost all experiments are more than two times higher than the amount of normal charge' [12, 13].

Although the volume of the fracture zone in the fracture form when detonating the concentric hemisphere concave shape charge was only 2 times higher than that of the concentrated explosion, the corresponding maximum specific energy value was 4.5 times. This difference reflects the excess energy of the concentric hemispherical shape charge, which increases the number of cracks and shows a wider crack width in the concrete sample compared with the concentrated charge.

When conducting experiments with the type of concave cylindrical charge with conical lining with angle at the top of funnel 78°, having the same volume of plastic explosive C4 is 40 g and tested to destroy concrete samples under the same conditions as described in above, the average value of 3 experimental samples was obtained: the volume of the funnel destroy $V_n = 567\ \text{cm}^3$. The average volume of the total sample destruction by crack is $V_k = 51{,}466\ \text{cm}^3$ [4]. The comparison of the volume of the destruction areas of the concentric hemispherical concave volume with the number of cylindrical shape charge with a conical-shaped hopper showed that the value of the destruction funnel area of the concentric amount of the larger hemispherical concave was approximately 4.8 times higher than the amount of the cylindrical concave explosion with the conical concave. The mean volume of the entire sample destruction in the cracks of the hemispherical shape charge was approximately 2 times smaller than that of the

cylindrical concave with the conical concave. This result again showed that the volume of the concave- and funnel-shaped blast has a better destruction rate of the explosion area than the conical-shaped cone. The shape charge with a conical lining had a higher energy concentration and transmitted deeper than the amount of the concave-shaped hemispherical funnel.

6 Conclusions

The following conclusions are drawn from this study:

- Using the principle of the concentric concave hemispherical shape charge allowed the increase of the coefficient of useful explosive energy and explosive force in the direction toward the rock surface to be broken. With this shape charge (case 3), the efficiency of the concentric shape charge was 45.12%, which is 2.7 times higher than the concentrated charge with the same explosive mass. Although the power of the selected hemispherical concave shape charge was reduced by approximately 3 times smaller than the concentrated charge, the area of the explosive effect was reduced because of the effect of the energy convergence of the lining funnel in the shape charge, which increased the explosive effect of the shape charge.
- The selected configuration of the concentric concave blasts $\overline{H} = 0.5$ and $\eta_d = 0.67$ corresponding to the outer hemisphere height is half the diameter and the radius of the inner crest (i.e., 0.67 out).
- By dint of the high efficiency and the increase of the explosive power of the shape charge, the volume of the destruction zone increased because of the direct effect of the explosion pulse and the compression wave 2 times destruction areas of the concentrated charge, when burst to break the grade M300 concrete sample.
- The value of stress and deformation in the concrete samples caused by the impact of the concave explosion was approximately 2.2 times higher than the effect of the concentrated detonation.
- The maximum specific energy value in the concrete sample caused by the effect of the concave shape charge was approximately 4.5 times higher than that of the concentrated charge.
- The results of the theoretical and empirical studies emphasised that the application of a concentric hemispherical shape charge will increase the efficiency of breaking out of rock by using external chargeswhen using contact explosion by a common concentrated charge.

Recommendation: We recommend the usage of the uniform parameters of the concentric hemisphere shape charge in case 3 to design and manufacture various types of final explosive with different capacities for rock and soil destruction on land or underwater. The calculated geometric parameters of the other capacity charge will be equal to the size of the shaped charge model multiplied by the explosive uniformity factor.

References

1. Giao, H.S., Thang, D.T., Quyen, L.V., Chung, H.T.: Chemical explosion - theory and practice, pp. 149–154, 239–245, 413–424. Scientific and Technical Publishing House, Hanoi (2010). (in Vietnamese)
2. Tan, T.B., Doanh, T.V.: The method of calculating the force of theconcave bullet concern the detonation position. J. Sci. Technol. MTA, Hanoi (2016). (in Vietnamese)
3. Charter of explosive work, pp. 113–118. Command of the Engineers, Hanoi (1986). (in Vietnamese)
4. Thang, D.T., Doanh, T.V., Viet, T.D., Tho, T.D.: Study on the reasonable parameters of the cylinder shaped charge with tapered liner funnel to destroy stone. In: International Symposium on Rock Mechanics and Engineering – The 35th VSRM Anniversary ISRM 2019 Specialized Conference, 22–24 November 2019, Hanoi, pp. 118–130 (2019)
5. Баум, Ф.А., Станюкович, К.П., Шехтер, Б.И.: Физика взрыва, pp. 367–440,629–637. Гасударственное издательство физико-математической литературы, Москва (1975)
6. Власов, О.Е.: Основы терии действия взрыва. ВИА, Москва (1957)
7. Барон, В.Л., Кантор, В.Х.: Техника и технология взрывных работ в США. Недра, Москва (1989)
8. Галкин, В.В., Гильманов, Р.А., Дроговейко, И.З.: Взрывные работы под водой. Недра, Москва (1987)
9. Покровский, Г.И.: Взрыв, pp. 48–56. Недра, Москва (1980)
10. Саламахин, Т.М.: Пособие для решения по теории механического действия взрыва, pp. 24–55, 98–99. ВИА, Москва (1967)
11. Руководство для инженерных воиск – подрывные работы, pp. 23–39, 371–384. Военно издательство министерства обороны союза СССР, Москва (1959)
12. Ханукаев, А.Н.: Физические процессы при отбойке горных пород взрывом, pp. 161–166. Недра, Москва (1974)
13. Софронов, А.А., Тачев, А.А.: Разрушение горных пород энергией взрыва кумулятивных зарядов – Проблема разрушения горных пород взрывом, pp. 189–198. Недра, Москва (1967)
14. Surface drilling and blasting, pp. 258–278. Tamrock (2001)
15. Explosives and demolition. Department of the army. Washington (1967)
16. Drilling and blasting of rocks, pp. 272–280. Geomining technological institute of Spain (1995)
17. Henrych, J.: The dynamic of explosion and its use, pp. 105–137, 278–295. Academia Prague (1979)
18. Olofsson, S.: Applied explosives technology for construction and mining, pp. 242–257. PrintedbyNoraBoktryckeriABNora (1975)
19. Кутузов, Б.Н.: Разрушение горных пород взрывом - Взрывные технологии в промышленности. МГГУ, Москва, 450 с (1994)
20. Руководство по подрывным работам, pp. 21–37, 371–384. Военно издательство министерства обороны союза СССР, Москва (1969)
21. Саламахин, Т.М.: Разрушнение взрывом элементов конструкций. ВИА, Москва (1967)
22. Evaluation of dynamic modulus of elasticity of concrete using impact – echo method published in Construction and Building materials 47(20133), 231–239